Chapter 11

Strong-Coupling Calculation of Fluctuation Pressure of a Membrane Between Walls

We calculate analytically the proportionality constant in the pressure law of a membrane thermally fluctuating between parallel walls from the strong-coupling limit of variational perturbation theory up to third order. Extrapolating these approximants to infinite order yields the pressure constant $\alpha = 0.0797149$ [48]. This result lies well within the error bounds of the most accurate available Monte Carlo result $\alpha_{\rm GK}^{\rm MC} = 0.0798 \pm 0.0003$ [88].

11.1 Membrane Between Walls

The violent thermal out-of-plane fluctuations of a membrane between parallel walls generate a pressure p following the law

$$p = \alpha \frac{k_B^2 T^2}{\kappa (d/2)^3}, \tag{11.1}$$

whose form was first derived by Helfrich [50] using dimensionality arguments. Here, κ denotes the elasticity constant of the membrane, and d the distance between the walls. The exact value of the prefactor α is unknown, but estimates have been derived from crude theoretical approximations by Helfrich [50] and by Janke and Kleinert [85], which yielded

$$\alpha_{\rm H}^{\rm th} \approx 0.0242, \quad \alpha_{\rm JK}^{\rm th} \approx 0.0625. \tag{11.2}$$

More precise values were found from Monte Carlo simulations by Janke and Kleinert [85] and by Gompper and Kroll [88], which gave

$$\alpha_{\rm JK}^{\rm MC} \approx 0.079 \pm 0.002, \quad \alpha_{\rm GK}^{\rm MC} \approx 0.0798 \pm 0.0003. \tag{11.3}$$

In a previous work [89], a systematic method was developed for calculating α with any desired high accuracy. Basis for this method is the strong-coupling version of variational perturbation theory [4]. The application of this method to the fluctuation pressure of the membrane is similar to that for the

particle in a box developed in Ref. [95]. In that theory, the free energy of the membrane is expanded into a sum of connected loop diagrams, which is eventually taken to infinite coupling strength to account for the hard walls. As a first approximation, an infinite set of diagrams was calculated, others were estimated by invoking a mathematical analogy with a similar one-dimensional system of a quantum mechanical particle between walls. The result of this procedure was a pressure constant

$$\alpha_{\mathrm{K}}^{\mathrm{th}} = \frac{\pi^2}{128} = 0.0771063\ldots, \tag{11.4}$$

very close to (11.3).

It is the purpose of this paper to go beyond this estimate by calculating all diagrams up to four loops exactly. In this way, we improve the analytic approximation (11.4) and obtain a value

$$\alpha^{\mathrm{th}} \approx 0.0797149, \tag{11.5}$$

which is in excellent agreement with the precise MC value $\alpha_{\mathrm{GK}}^{\mathrm{MC}}$ in Eq. (11.3).

11.2 Smooth Potential Model of Membrane Between Walls

To set up the theory, we let the membrane lie in the $\mathbf{x}$-plane and fluctuate in the z-direction with vertical displacements $\varphi(\mathbf{x})$. The walls at $z = \pm d/2$ restrict the displacements to the interval $\varphi(\mathbf{x}) \in (-d/2, d/2)$. Near zero temperature, the thermal fluctuations are small, $\varphi(\mathbf{x}) \approx 0$. The curvature energy E_C of the membrane has the harmonic approximation (10.54)

$$E_C = \frac{1}{2}\kappa \int dx^2\, [\partial^2 \varphi(\mathbf{x})]^2. \tag{11.6}$$

The thermodynamic partition function Z of the membrane is given by the sum over all Boltzmann factors of field configurations $\varphi(\mathbf{x})$

$$Z = \prod_{\mathbf{x}} \left[\int_{-d/2}^{+d/2} \frac{d\varphi(\mathbf{x})}{\sqrt{2\pi k_B T/\kappa}} \right] \exp\left\{ -\frac{\kappa}{2k_B T} \int d^2x\, [\partial^2 \varphi(\mathbf{x})]^2 \right\}. \tag{11.7}$$

This simple harmonic functional integral poses the problem of dealing with a finite range of fluctuations. This problem is solved by the strong-coupling theory of Ref. [89] as follows.

If the area of the membrane is denoted by A, the partition function (11.11) determines the free energy per area as

$$f = -\frac{1}{A} \ln Z. \tag{11.8}$$

By differentiating f with respect to the distance d of the walls, we obtain the pressure $p = -\partial f/\partial d$.

11.2.1 Smooth Potential Adapting Walls

We introduce some smooth potential restricting the fluctuations $\varphi(\mathbf{x})$ to the interval $(-d/2, d/2)$, for instance

$$V(\varphi(\mathbf{x})) = m^4 \frac{d^2}{\pi^2} \tan^2 \frac{\pi}{d}\varphi(\mathbf{x}) \equiv m^4 \varphi^2(\mathbf{x}) + \frac{\pi^2}{d^2} V_{\mathrm{int}}(\varphi(\mathbf{x})), \tag{11.9}$$

where we have split the potential into a harmonic and an interacting part

$$V_{\mathrm{int}}(\varphi(\mathbf{x})) = m^4 \left[\varepsilon_4 \varphi^4(\mathbf{x}) + \varepsilon_6 \left(\frac{\pi}{d}\right)^2 \varphi^6(\mathbf{x}) + \varepsilon_8 \left(\frac{\pi}{d}\right)^4 \varphi^8(\mathbf{x}) + \ldots \right] \tag{11.10}$$

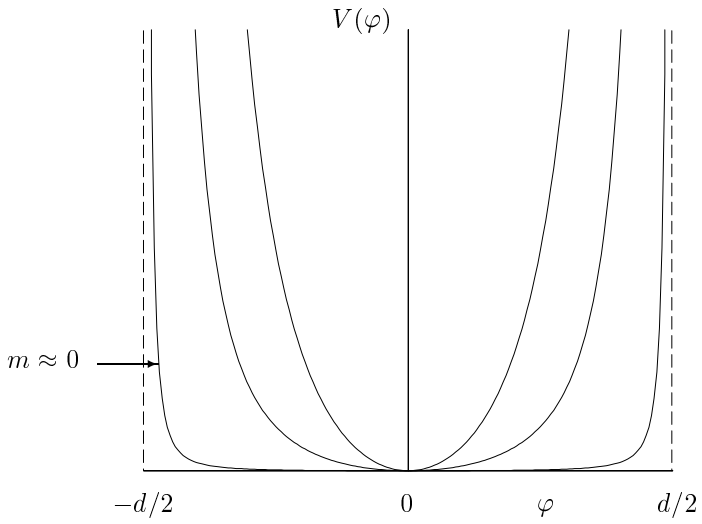

FIGURE 11.1: Smooth potential $V(\varphi)$ for different values of the parameter m. In the limit $m \to 0$ the hard walls at $\varphi = \pm d/2$ are adapted.

with $\varepsilon_4 = 2/3, \varepsilon_6 = 17/45, \varepsilon_8 = 62/315, \ldots$. Thus we are left with the functional integral

$$Z = \oint \mathcal{D}\varphi(\mathbf{x}) \exp\left(-\frac{1}{2}\int d^2x \left\{[\partial^2\varphi(\mathbf{x})]^2 + m^4\varphi^2(\mathbf{x}) + \frac{\pi^2}{d^2}V_{\text{int}}(\varphi(\mathbf{x}))\right\}\right), \tag{11.11}$$

where we have set $\kappa = k_BT = 1$. After truncating the Taylor expansion around the origin, the periodicity of the trigonometric function is lost and the integrals over $\varphi(\mathbf{x})$ in (11.7) can be taken from $-\infty$ to $+\infty$. The interacting part is treated perturbatively. Then, the harmonic part of $V(\varphi(\mathbf{x}))$ leads to an exactly integrable partition function Z_{m^2}. The mass parameter m is arbitrary at the moment, but will eventually be taken to zero, in which case the potential $V(\varphi(\mathbf{x}))$ describes two hard walls at $\varphi = \pm d/2$. Figure 11.1 illustrates this behavior of the potential.

We shall now calculate a perturbation expansion for Z up to four loops. This will serve as a basis for the limit $m \to 0$, which will require the strong-coupling theory of Ref. [89].

11.2.2 Perturbation Expansion for Free Energy

The perturbation expansion proceeds from the harmonic part of Eq. (11.11):

$$Z_{m^2} = \oint \mathcal{D}\varphi(\mathbf{x})\, e^{-\mathcal{A}_{m^2}[\varphi]} = e^{-Af_{m^2}} \tag{11.12}$$

with

$$\mathcal{A}_{m^2}[\varphi] = \frac{1}{2}\int d^2x \left\{[\partial^2\varphi(\mathbf{x})]^2 + m^4\varphi^2(\mathbf{x})\right\}. \tag{11.13}$$

From Refs. [85,89], the harmonic free energy per unit area f_{m^2} is known as

$$f_{m^2} = \frac{1}{8}m^2. \tag{11.14}$$

The harmonic correlation functions associated with (11.12) are

$$\langle O_1(\varphi(\mathbf{x}_1))\, O_2(\varphi(\mathbf{x}_2))\, \cdots\rangle_{m^2} = \frac{1}{Z_{m^2}} \oint \mathcal{D}\varphi(\mathbf{x}) O_1(\varphi(\mathbf{x}_1))\, O_2(\varphi(\mathbf{x}_2)) \cdots e^{-\mathcal{A}_{m^2}[\varphi]}, \tag{11.15}$$

where the functions $O_i(\varphi(\mathbf{x}_j))$ may be arbitrary polynomials of $\varphi(\mathbf{x}_j)$. The basic harmonic correlation function

$$G_{m^2}(\mathbf{x}_1, \mathbf{x}_2) = \langle \varphi(\mathbf{x}_1)\, \varphi(\mathbf{x}_2) \rangle_{m^2} \tag{11.16}$$

determines, by Wick's rule, all correlation functions (11.15) as sums of products of (11.16):

$$\langle \varphi(\mathbf{x}_1) \cdots \varphi(\mathbf{x}_n) \rangle_{m^2} = \sum_{\text{pairs}} G_{m^2}(\mathbf{x}_{P(1)}, \mathbf{x}_{P(2)}) \cdots G_{m^2}(\mathbf{x}_{P(n-1)}, \mathbf{x}_{P(n)}), \tag{11.17}$$

where the sum runs over all pair contractions, and P denotes the associated index permutations. The harmonic correlation function (11.16) reads in momentum space

$$G_{m^2}(\mathbf{k}) = \frac{1}{k^4 + m^4} = \frac{i}{2m^2} \left[\frac{1}{k^2 + im^2} - \frac{1}{k^2 - im^2} \right], \tag{11.18}$$

thus being proportional to the difference of two ordinary correlation functions $(p^2 - \mu^2)^{-1}$ with an imaginary square mass $\mu^2 = \pm i m^2$. From their known $\mathbf{x}$-space form we have immediately

$$G_{m^2}(\mathbf{x}_1, \mathbf{x}_2) = G_{m^2}(\mathbf{x}_1 - \mathbf{x}_2) = \frac{i}{4\pi m^2} \left[K_0(\sqrt{i} m |\mathbf{x}_1 - \mathbf{x}_2|) - K_0(\sqrt{-i} m |\mathbf{x}_1 - \mathbf{x}_2|) \right], \tag{11.19}$$

where $K_0(z)$ is a modified Bessel function [96, Section 8.432]. At zero distance, the ordinary harmonic correlations are logarithmically divergent, but the difference is finite yielding $G_{m^2}(0) = 1/8m^2$.

We now expand the partition function (11.11) in powers of $g V_{\text{int}}(\phi(\mathbf{x}))$, where $g \equiv \pi^2/d^2$, and use the expectation values (11.15) to obtain a perturbation series for Z. Going over to the cumulants, we find the free energy per unit area

$$f = f_{m^2} + \frac{g}{2A} \int d^2x \langle V_{\text{int}}(\varphi(\mathbf{x})) \rangle_{m^2,c} - \frac{g^2}{2!} \frac{1}{4A} \int d^2x_1 d^2x_2 \langle V_{\text{int}}(\varphi(\mathbf{x}_1)) V_{\text{int}}(\varphi(\mathbf{x})_2) \rangle_{m^2,c} + \dots, \tag{11.20}$$

where the subscript c indicates the cumulants. Inserting the expansion (11.10) and using (11.15) as well as (11.17), the series can be written as

$$f = m^2 \left[a_0 + \sum_{n=1}^{\infty} a_n \left(\frac{g}{m^2} \right)^n \right], \tag{11.21}$$

where the coefficients a_n are dimensionless real numbers, starting with $a_0 = 1/8$ from Eq. (11.14). The higher expansion coefficients a_n are combinations of integrals over the connected correlation functions:

$$a_1 = \varepsilon_4 \frac{m^4}{2A} \int d^2x \, \langle \varphi^4(\mathbf{x}) \rangle_{m^2,c}, \tag{11.22}$$

$$a_2 = \varepsilon_6 \frac{m^6}{2A} \int d^2x \, \langle \varphi^6(\mathbf{x}) \rangle_{m^2,c} - \varepsilon_4^2 \frac{m^{10}}{8A} \int d^2x_1 d^2x_2 \, \langle \varphi^4(\mathbf{x}_1)\, \varphi^4(\mathbf{x}_2) \rangle_{m^2,c}, \tag{11.23}$$

$$\begin{aligned} a_3 = {} & \varepsilon_8 \frac{m^8}{2A} \int d^2x \, \langle v^8(\mathbf{x}) \rangle_{m^2,c} - \varepsilon_4 \varepsilon_6 \frac{m^{12}}{4A} \int d^2x_1 d^2x_2 \, \langle \varphi^6(\mathbf{x}_1)\, \varphi^4(\mathbf{x}_2) \rangle_{m^2,c} \\ & + \varepsilon_4^3 \frac{m^{16}}{48A} \int d^2x_1 d^2x_2 d^2x_3 \langle \varphi^4(\mathbf{x}_1) \varphi^4(\mathbf{x}_2) \varphi^4(\mathbf{x}_3) \rangle_{m^2,c}. \end{aligned} \tag{11.24}$$

To find the free energy (11.21) between walls, we must go to the limit $m^2 \to 0$. Following [4,89], we substitute m^2 by the variational parameter M^2, which is introduced via the trivial identity

$$m^2 \equiv \sqrt{M^4 - gr} \tag{11.25}$$

with

$$r = \frac{1}{g} \left(M^4 - m^4 \right), \tag{11.26}$$

and expand the r.h.s. of Eq. (11.25) in powers of g up to the order g^N. In the limit $m^2 \to 0$, this expansion reads

$$m^2(M^2) = M^2 - \frac{1}{2}\frac{r}{M^2}g - \frac{1}{8}\frac{r^2}{M^6}g^2 - \frac{1}{16}\frac{r^3}{M^{10}}g^3 - \dots . \tag{11.27}$$

Inserting this into (11.21), re-expanding in powers of g, re-substituting r from Eq. (11.26), and truncating after the Nth term, we arrive at the free energy per unit area

$$f_N(M^2, d) = M^2\, a_0\, b_0 + \sum_{n=1}^{N} a_n g^n M^{2(1-n)} b_n, \tag{11.28}$$

with

$$b_n = \sum_{k=0}^{N-n} (-1)^k \begin{pmatrix} (1-n)/2 \\ k \end{pmatrix} \tag{11.29}$$

being the binomial expansion of $(1-1)^{(1-n)/2}$ truncated after the $(N-n)$th term [89]. The optimization of (11.28) is done as usual [4] by determining the minimum of $f_N(M^2, d)$ with respect to the variational parameter M^2, i.e. by the condition

$$\frac{\partial f_N(M^2, d)}{\partial M^2} \stackrel{!}{=} 0, \tag{11.30}$$

whose solution gives the optimal value $M_N^2(d)$. Re-substituting this result into Eq. (11.28) produces the optimized free energy $f_N(d) = f_N(M_N^2(d), d)$, which only depends on the distance as $f_N(d) = 4\alpha_N/d^2$. Its derivative with respect to d yields the desired pressure law with the Nth-order approximation for the constant α_N:

$$p_N = \alpha_N \left(\frac{d}{2}\right)^{-3}. \tag{11.31}$$

We must now calculate the cumulants occurring in the expansion (11.21).

11.3 Evaluation of the Fluctuation Pressure up to Four-Loop Order

The correlation functions appearing in (11.22)–(11.24) are conveniently represented by Feynman graphs. Green functions are pictured as solid lines and local interactions as dots, whose coordinates are integrated over:

$$\mathbf{x}_1 \text{ —— } \mathbf{x}_2 \equiv G_{m^2}(\mathbf{x}_1, \mathbf{x}_2), \tag{11.32}$$

$$\bullet \equiv \int d^2x. \tag{11.33}$$

These rules can be taken over to momentum space in the usual way. One easily verifies that the integrals over the connected correlation functions in (11.22)–(11.24) have a dimension $A/m^{2(l+V-1)}$, where V is the number of the vertices and l denotes the number of lines of the associated Feynman diagrams. Thus we parameterize each Feynman diagram by $vA/m^{2(l+V-1)}$, with a dimensionless number v, which includes the multiplicity. In Table 11.1, we have listed the values v for all diagrams up to four loops. No divergences are encountered. Exact results are stated as fractional numbers. The other numbers are obtained by numerical integration, which are reliable up to the last written digit. The right-hand column shows numbers v_{K} obtained by the earlier approximation [89], where all the Feynman diagrams were estimated by an analogy to the the problem of a particle in a box. In Ref. [89],

TABLE 11.1: Feynman diagrams with loops L, multiplicities s, and their dimensionless values v. The last column shows the values $v_{\rm K} = v_{\rm PB}/4^L$ used in Ref. [89].

L	Graph	s	v	$v_{\rm K}$
2		3	$\frac{3}{64}$	$\frac{3}{64}$
			$a_1 = a_1^{\rm K}$	$a_1^{\rm K} = 1/64$
3		15	$\frac{15}{512}$	$\frac{15}{512}$
	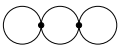	72	$\frac{9}{128}$	$\frac{9}{128}$
		24	$0.828571 \times \frac{3}{256}$	$\frac{3}{256}$
			$a_2 = 1.114286\, a_2^{\rm K}$	$a_2^{\rm K} = 1/1024$
4		105	$\frac{105}{4096}$	$\frac{105}{4096}$
	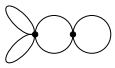	540	$\frac{135}{2048}$	$\frac{135}{2048}$
	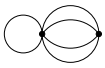	360	$0.828571 \times \frac{45}{2048}$	$\frac{45}{2048}$
	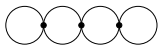	2592	$\frac{81}{512}$	$\frac{81}{512}$
	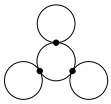	1728	$\frac{81}{512}$	$\frac{81}{512}$
	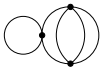	3456	$0.828571 \times \frac{135}{1024}$	$\frac{135}{1024}$
		1728	$0.713194 \times \frac{81}{2048}$	$\frac{81}{2048}$
			$a_3 = 2.763097 \cdot 10^{-5}$	$a_3^{\rm K} = 0$

it was shown that the value v of a large class of diagrams of the membrane problem can be obtained by simply dividing the value of the corresponding particle-in-a-box-diagram $v_{\rm PB}$ by a factor $1/4^L$, where L is the number of loops in the diagrams.

Inserting the numbers in Table 11.1 into (11.22)–(11.24), we obtain the coefficients a_1, a_2, a_3 of the free energy per area (11.28), which is then extremized in M^2. To see how the results evolve from order to order, we start with the first order

$$f_1(M^2, d) = \frac{1}{2} a_0 M^2 + a_1 \frac{\pi^2}{d^2} \tag{11.34}$$

with $a_0 = 1/8$ and $a_1 = 1/64$. Here, an optimal value of M^2 does not exist. Thus we simply use the perturbative result for $m = 0$, which is equal to (11.34) for $M = 0$. Differentiating $f_1(0, d)$ with respect to d yields the pressure constant in (11.31):

$$\alpha_1 = \frac{1}{4} a_1 \frac{\pi^2}{d^2} = \frac{\pi^2}{256} \approx 0.038553. \tag{11.35}$$

This value is about half as big as the Monte Carlo estimates (11.3) and agrees with the value found

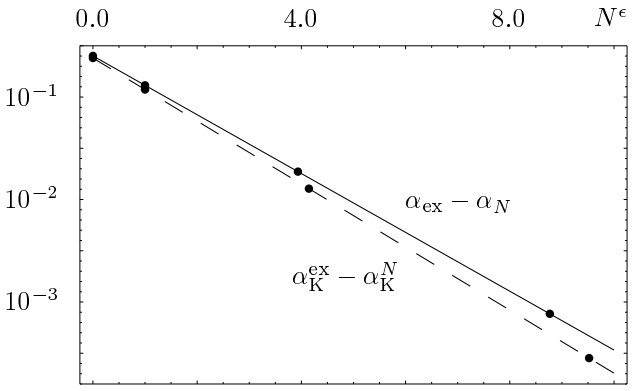

FIGURE 11.2: Difference between the extrapolated pressure constant $\alpha_{\rm ex}$ and the optimized N-th order value α_N obtained from variational perturbation theory for the method presented in this chapter (solid line) and the first four values of the approximation scheme introduced in Ref. [89] (dashed line). Dots represent the values to order N in these approximations.

in [89]. To second order, the re-expansion (11.28) reads

$$f_2(M^2, d) = \frac{3}{8} a_0 M^2 + a_1 \frac{\pi^2}{d^2} + a_2 \frac{\pi^4}{d^4} \frac{1}{M^2} \tag{11.36}$$

with $a_2 \approx 1.0882 \cdot 10^{-3}$ from Table 11.1. Minimizing this free energy in M^2 yields an optimal value

$$M_2^2(d) = \sqrt{\frac{8}{3} \frac{a_2}{a_0}} \frac{\pi^2}{d^2} \approx 0.152362 \frac{\pi^2}{d^2}, \tag{11.37}$$

and

$$f_2(d) = \frac{\pi^2}{d^2} \left(a_1 + \sqrt{\frac{3}{2} a_0 a_2} \right). \tag{11.38}$$

Inserting $a_0 = 1/8$ and a_1, a_2 from Table 11.1, we obtain

$$\alpha_2 \approx 0.073797, \tag{11.39}$$

thus improving drastically the first-order estimate (11.35). This value is by a factor 1.026 larger than that obtained in the approximation of Ref. [89].

Continuing this proceeding to third order, we must minimize

$$f_3(M^2, d) = \frac{5}{16} a_0 M^2 + a_1 \frac{\pi^2}{d^2} + \frac{3}{2} a_2 \frac{\pi^4}{d^4} \frac{1}{M^2} + a_3 \frac{\pi^6}{d^6} \frac{1}{M^4} \tag{11.40}$$

with $a_3 \approx 2.7631 \cdot 10^{-5}$. The optimal value of M^2 is

$$M_3^2(d) = \sqrt{\frac{32}{5} \frac{a_2}{a_0}} \cos \left[\frac{1}{3} \arccos \sqrt{\frac{5}{2} \frac{a_0 a_3^2}{a_2^3}} \right] \frac{\pi^2}{d^2} \approx 0.219608 \frac{\pi^2}{d^2}. \tag{11.41}$$

Inserted into (11.40), we find the four-loop approximation for the proportionality constant α:

$$\alpha_3 \approx 0.079472. \tag{11.42}$$

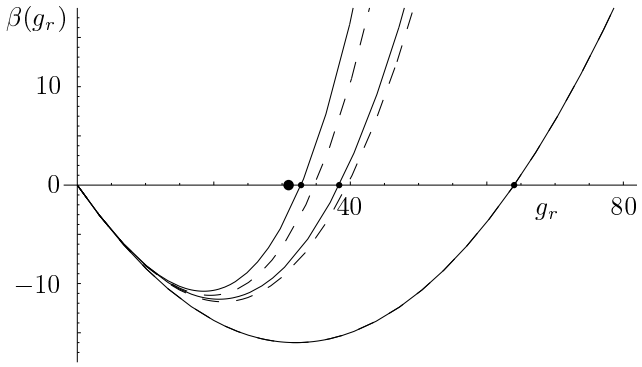

FIGURE 11.3: Plot of successive β-like functions associated with expansion (11.46) to orders $N = 1, 2, 3$ (solid curves). For comparison, we also plot the corresponding functions obtained from the approximate expansion coefficients a_n^{K} (dashed curves). The curves coincide for $N = 1$. The zeros $g_{r,N}^\star$ of the Nth approximation are from right to left: $g_{r,1}^\star = 64$ (64), $g_{r,2}^\star = 38.369$ (39.554), and $g_{r,3}^\star = 32.783$ (34.796). The zeros approach rapidly the value $g_r^\star = 30.953$ (fat dot) associated with the pressure constant (11.45).

This result is in very good agreement with the Monte Carlo results in (11.3) and should be a lower bound for the exact value since the successive approximations increase monotonously with the order of the approximation. It differs from the approximate value of the method presented in Ref. [89] by a factor 1.047.

An even better result will now be obtained by extrapolating the sequence $\alpha_1, \alpha_2, \alpha_3$ to infinite order.

11.4 Extrapolation Towards the Exact Constant

Variational perturbation theory exhibits typically an exponentially fast convergence. This was exactly proven for the anharmonic oscillator [4]. Other systems treated by variational perturbation theory show a similar behavior [53]. Assuming that an exponential convergence exists also here, we may extrapolate the sequence of values $\alpha_1, \alpha_2, \alpha_3$ calculated above to infinite order. It is useful to extend this sequence by one more value at the lower end, $\alpha_0 = 0$, which follows from the one-loop energy (11.14) at $m^2 = 0$. This sequence is now extrapolated towards a hypothetical exact value α_{ex} by parameterizing the approach as

$$\alpha_{\mathrm{ex}} - \alpha_N = \exp\left(-\eta - \xi N^\epsilon\right). \tag{11.43}$$

The parameters η, ξ, ε, and the unknown value of α_{ex} are determined from the four values $\alpha_0, \ldots, \alpha_3$, with the result

$$\eta = 2.529298, \quad \xi = 0.660946, \quad \epsilon = 1.976207, \tag{11.44}$$

and the extrapolated value for the exact constant:

$$\alpha_{\mathrm{ex}} = 0.0797149. \tag{11.45}$$

This is now in perfect agreement with the Monte Carlo values (11.3).

The approach is graphically shown in Fig. 11.2, where the optimized values $\alpha_0, \ldots, \alpha_3$ all lie on a straight line (solid line). For comparison, we have also extrapolated the first four values $\alpha_{\mathrm{K}}^0, \ldots, \alpha_{\mathrm{K}}^3$ in the approach of Ref. [89] yielding a value $\alpha_{\mathrm{exK}} \approx 0.0759786$, which is 4.9% smaller than (11.45).

11.5 Comparison with the Renormalization Group Approach

Rewriting the perturbation series (11.21) as $f = [g_r(\tilde{g})]^{-1}\pi^2/d^2$ with the dimensionless function

$$g_r(\tilde{g}) = \tilde{g}(a_0 + a_1\tilde{g} + a_2\tilde{g}^2 + a_3\tilde{g}^3 + \dots)^{-1} = \frac{1}{a_0}\left[\tilde{g} - \frac{a_1}{a_0}\tilde{g}^2 + \left(\frac{a_1^2}{a_0^2} - \frac{a_2}{a_0}\right)\tilde{g}^3 + \dots\right] \tag{11.46}$$

of the reduced coupling constant $\tilde{g} = g/m^2$, its logarithmic derivative $s(\tilde{g}) = \partial \log g_r(\tilde{g})/\partial \log \tilde{g}$ vanishes at infinitively strong coupling since $g_r(\tilde{g} \to \infty) = g_r^\star = \text{const}$. This constant determines the pressure constant as

$$\alpha = \frac{\pi^2}{4}[g_r^\star]^{-1}. \tag{11.47}$$

In analogy to the renormalization group method in field theory, we may now define a β-like function by $\beta(\tilde{g}) = -g_r(\tilde{g})s(\tilde{g})$, as done in Ref. [97]. Since this function vanishes in the limit of infinitely strong coupling $\tilde{g} \to \infty$, we invert the series (11.46) for $\tilde{g}(g_r)$ and re-expand the β-like function in powers of g_r obtaining $\beta(g_r)$. This function vanishes at the value $g_r^\star$ determining once more the pressure constant via Eq. (11.47). The terms in Eq. (11.46) yield successively the values $\alpha_1 = 0.038553, \alpha_2 = 0.064308, \alpha_3 = 0.075265$, which approach the estimate (11.45). Figure 11.3 shows the first three β-like functions for different orders and their zeros together with the zero corresponding to our value (11.45).